Formally published as:

Title:


Performance Comparison of Conventional and Amorphous AM-Built PMSM, 2024 International Conference on Electrical Machines (ICEM), Torino, Italy, 2024, pp. 1-7, doi: 10.1109/ICEM60801.2024.10700548.


Authors:


C. Klein, L. Thorsson, C. May, M. Nienhaus

# Performance Comparison of Conventional and Amorphous AM-built PMSM

Klein Carsten
*Laboratory of Actuation Technology*
*Saarland University*
Saarbrücken, Germany
klein@lat.uni-saarland.de

Thorsson Lena
*Heraeus AMLOY Technologies GmbH*
Karlstein am Main, Germany
lena.thorsson@addmira.se

May Christopher
*Laboratory of Actuation Technology*
*Saarland University*
Saarbrücken, Germany
may@lat.uni-saarland.de

Nienhaus Matthias
*Laboratory of Actuation Technology*
*Saarland University*
Saarbrücken, Germany
nienhaus@lat.uni-saarland.de

***Abstract*—The performance of additively manufactured electrical machines could see improvement through the utilization of iron-based amorphous materials. These materials exhibit a notable combination of high magnetic permeability and increased specific electrical resistance, albeit with a lower saturation flux density compared to conventional electrical steel. In this study, two identical permanent magnet synchronous machines (PMSMs) are compared, differing only in their soft-magnetic components (SMCs). While one PMSM incorporates electrical steel, the other utilizes bulk metallic glass (BMG) fabricated via selective laser melting (SLM). The BMG-based machine demonstrates a noteworthy reduction in torque output at equal current levels, yet it exhibits superior efficiency under certain operating conditions compared to its electrical steel counterpart. Moreover, the temperature of the BMG-based machine tends to be higher than that of the sheet-based machine.**

***Index Terms*—Additive Manufacturing, Bulk Metallic Glass, PMSM, Electrical Machine**

## I. Introduction

Electrical machine manufacturing is currently being extended with the integration of additive manufacturing (AM) techniques. In particular, soft-magnetic components (SMCs) used to guide the magnetic flux have been manufactured using AM [1] and some research expands on this by even manufacturing the electrical coils in this manner [2]. Although a number of AM techniques exist for the applied iron-based alloys, the main focus in research has been on laser powder bed fusion (LPBF) with most research groups employing selective laser melting (SLM) [3]–[5]. AM techniques in general allow for an increased flexibility in design compared to traditional techniques. Thus, novel machine designs based on three dimensional flux guidance may become feasible in the near future.

Another research topic of interest is the possibility of using soft-magnetic amorphous metals in electrical machines. Amorphous materials do not exhibit a long-range order and therefore do not have a crystalline structure which is otherwise common for metals. In order to achieve this non-crystalline state, a frequently used method is to cool the liquid metal rapidly [6]. Methods such as melt spinning have been used extensively to manufacture thin ribbons of amorphous metal [7] with thicknesses around 10 to $40\,\mu\mathrm{m}$ [8]. However, using these strips to manufacture large components is tedious and requires a lot of time and effort, which is why the only practical application is to wind these strips into simple structures such as toroids. More complex structures such as electrical machine components require additional manufacturing steps performed on these simple wound parts [9]. Already in these applications amorphous metals show benefits such as low losses and high permeabilities while still achieving competitive flux densities [10], [11]. Recent comparative studies such as [12], [13] have found amorphous SMCs to be especially efficient for medium frequencies while [14] has also shown an increase in efficiency compared to electrical steel sheets at ultra-high speed applications. In [15] it was shown that amorphous SMCs even outperform nanocrystalline materials concerning efficiency, although other aspects such as magnetic permeability are lower. With the aim of widening the realm of application, larger and more complex structures based on amorphous metals have to become more feasible to manufacture without requiring additional manufacturing steps.

In material science, alloys that due to their chemical composition have such good glass forming ability (GFA) that they maintain an amorphous microstructure also when manufactured in thicknesses larger than $1\,\mathrm{mm}$ are called bulk metallic glasses (BMGs) [16]. Accomplishing larger and more complex components that are solid and are not based on wound ribbons hence require using a suitable alloy in combination with an appropriate manufacturing technique.

SLM is a great candidate for this intent as it creates the geometry of the component and its amorphous microstructure simultaneously. The layerwise manufacturing where a fine-focused laser beam rapidly scans powder layers in the realm

This research was funded by the European Union's Horizon Europe Pathfinder-Open Programme grant number 101046870.

of $20\,\mu\mathrm{m}$ thickness means that only a small volume of material remains molten for a brief moment of time [17]. As the laser beam continues its travel, the cooling rate of the melted volume inherently reaches approximately $1 \times 10^4\,\mathrm{K/s}$ or more [5], which is sufficient for a BMG alloy to solidify into the desired amorphous microstructure. Thus, the component should be amorphous without the need of additional treatment. Therefore, this manufacturing technique is able to combine the benefits of both additive manufacturing as well as amorphous soft-magnetic materials.

In reality, however, there are additional challenges to successful manufacturing which have slowed down the industrialisation of the technique. First, the inherent brittleness that especially iron-based BMGs show makes the alloys sensitive to thermal and residual stresses that cannot be avoided during SLM processing. This typically results in cracking of the material, with crack patterns on both micro- and macrolevel, which has been reported by several research groups [5], [17], [18]. While it can be understood that cracks impair mechanical strength and change electromagnetic properties compared to theoretical values, their formation is still a novel topic of research [19]. This generally unpredictable nature of cracking poses a significant challenge to producing sound components and performing dependable simulations.

Second, while SLM is known to give repetitive quality regarding microstructure for crystalline metals, an added challenge for amorphous alloys is the importance of controlling the thermal history for a part through the full process chain. If the amorphous material becomes too hot for too long at any point, it might crystallize to some degree. Hence, for a certain alloy, an SLM process that produces fully amorphous samples of small size might result in a more crystallised material when a larger and more complex component with varying cross-sections is manufactured. Adjusting and documenting the SLM process for components of various sizes costs time and effort for application developers. Also, care has to be taken so that sufficient cooling is used for any heat-inducing post-processing steps such as cutting.

The present study provides a comparison of a Permanent Magnet Synchronous Machine (PMSM) made of laminated electrical steel sheets (Sheet-Machine) and one made of soft-magnetic BMG components manufactured using SLM (BMG-Machine). Chapter II introduces the soft-magnetic materials used for both machines and provides an overview of the manufacturing process as well as the PMSM design. After describing the test bench and applied test sequence, experimental results are presented and discussed in Chapter III. Finally, Chapter IV provides concluding remarks.

## II. PMSM and Manufacturing

The electrical machine used for the experimental investigation is a 16 pole, 18 slot PMSM with a single layer concentrated winding. A cross section of the CAD model is shown in Figure 1 while the resulting prototypes are shown in Figure 2. The data of the PMSM, which was designed for research on sensorless control, is summarized in Table I.

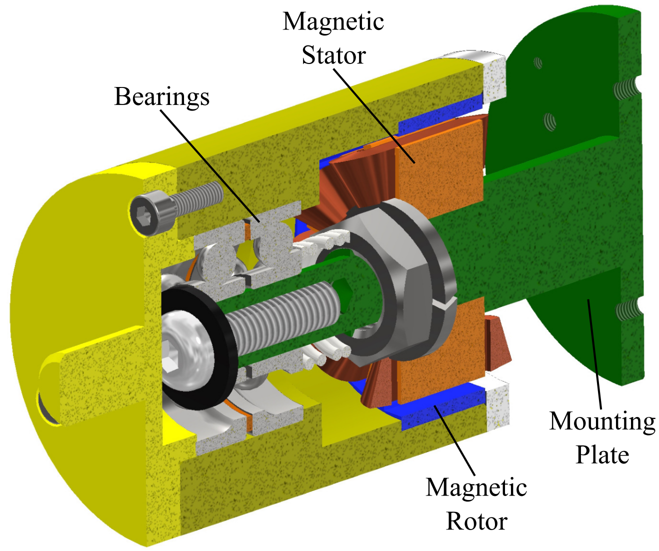


Fig. 1. Cross section of the CAD model of the PMSM used for the present experimental investigation.

Fig. 2. PMSMs used in the experimental investigation. **1**: BMG-Machine. **2**: Sheet-Machine.

TABLE I
DATA OF THE PMSM USED IN THIS STUDY.

| **Name** | **Value** |
|---|---|
| Number of poles | 16 |
| Number of slots | 18 |
| Winding Pattern | AbbCaaBcc |
| Winding Details | Concentrated Winding, Single Layer |
| Turns per Slot | 12 |
| Permanent Magnets | BMN-46SH/ST |
| Stack Length | 15 mm |
| Outer Diameter | 42 mm |
| Nominal Voltage | 24 V |
| Maximum Current | 12 A |

Both PMSMs are manufactured to be as identical as possible apart from the SMCs. These components have a nominal height of $15\,\mathrm{mm}$, although due to the necessity to use a natural number of sheets, tolerances and insulation, their true height is $14.8\,\mathrm{mm}$. The SMCs of the Sheet-Machine are made from electrical steel of type M 270-50 A, which is the material this PMSM was initially designed for. The individual sheets were cut using a laser cutting process. Their thickness is $0.5\,\mathrm{mm}$ such that 29 of them result in the rotor and stator, respectively. A bonding varnish was used to package the sheets to form the finished SMCs.

The BMG equivalents of both the rotor and the stator were manufactured using an SLM process and the commercially available powder Kuamet. The Kuamet powder is an iron-based soft-magnetic amorphous alloy that is marketed for electromagnetic applications. However, the alloy was developed for other manufacturing techniques than AM according to the supplier, and therefore some properties, such as GFA, are less than optimal for SLM. The BMG components were manufactured using a Trumpf TP1000 machine using previously developed parameters [5]. An example of the microstructure is shown in Figure 3. As the figure shows, the vertical microcracks are homogeneously distributed. Most cracks appear $100\,\mu\mathrm{m}$ to $200\,\mu\mathrm{m}$ in length in the 2D cross-cut while just a few micrometers in width. Also visible are process-related pores with rounded, organic shapes.

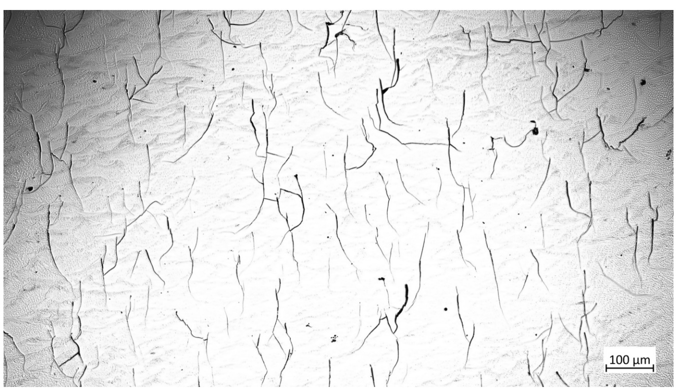


Fig. 3. Micrograph of the polished cross-cut of an SLM-processed BMG-sample. Building direction and microcracking direction are both vertical in the figure and hence parallel.

The BMG-based components were manufactured slightly higher than the nominal height and subsequently cut using wire electrical discharge machining to $14.8\,\mathrm{mm}$ in order to match the height of the sheet-based SMCs. The final components are shown in Figure 4 with the coils and permanent magnets already mounted. As can be seen on the outer diameter of the rotor, the surface of the components are quite rough, which may promote mechanical faults and likely deteriorates the magnetic performance slightly. The scraps from the cutting process were investigated using differential scanning calorimetry (DSC) with the aim of determining the amorphic fraction. The reference for the amorphic fraction is a fully amorphous ribbon of the same material which was additionally checked by means of X-ray diffraction. The rotor was measured to have an amorphic fraction of $68.0\%$ while that of the stator is $70.5\%$. Thus, while not fully amorphous, the overall effect of using amorphous instead of crystalline SMCs should be significant.

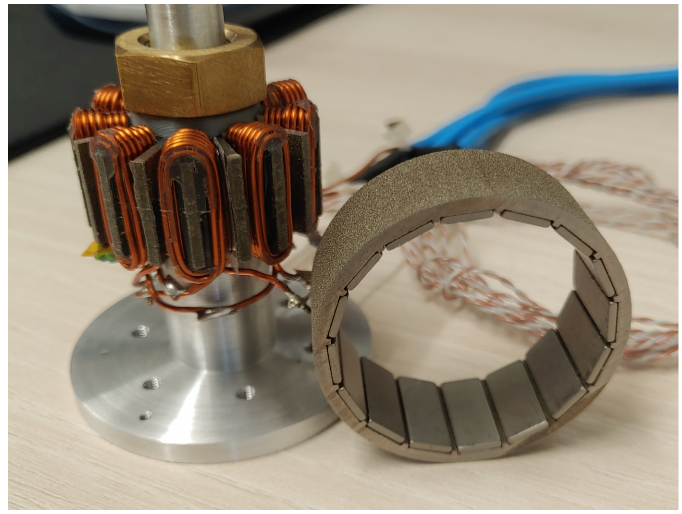

Fig. 4. Partially amorphous soft-magnetic components manufactured using SLM. The coils and permanent magnets are already mounted to the stator (left) and rotor (right) respectively.

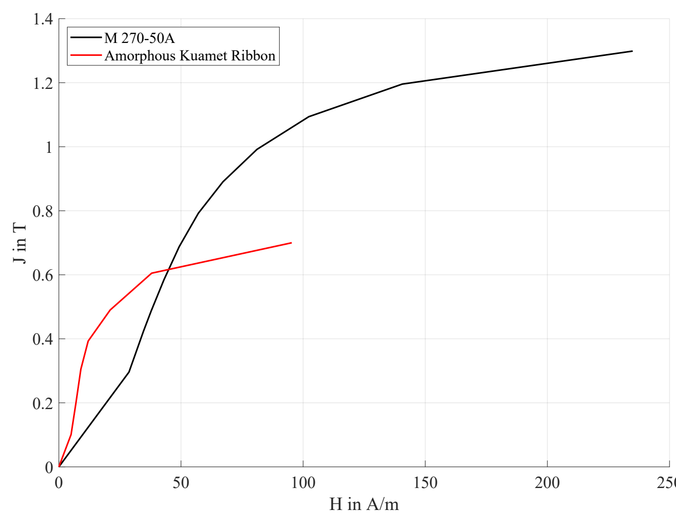


Fig. 5. Magnetic field strength H to polarization J characteristic of the fully amorphous Kuamet ribbon and the electrical steel of type M 270-50A used in the experimental investigation.

The relation of magnetic field strength and polarization of both materials is illustrated in Figure 5. The data for the electrical steel was provided by the manufacturer while the data for the BMG is based on magnetic measurements. The measurement setup is limited concerning the range of the applicable magnetic field strength which is why the data for the amorphous material is cut off at about $100\,\mathrm{A/m}$. It should be noted that the measurements were not performed on the rotor or stator material but rather on a fully amorphous ribbon made using melt spinning. Thus, the magnetic properties of the SMCs will likely deviate from the shown results. Due to the nature of the available samples, an open-circuit measurement had to be performed. The measurement setup itself is based on an actuation coil and a measurement coil.

Figure 5 clearly shows the high magnetic permeability of the amorphous material indicated by the increased slope compared to the electrical steel. However, the drawback of the material is also obvious as the bend in the H-J characteristic is already significant at $0.5\,\mathrm{T}$. This also results in a large difference in the saturation flux density which is about $1.93\,\mathrm{T}$ in the case of the electrical steel and only $1.33\,\mathrm{T}$ for the amorphous material. Therefore, one can expect the air gap flux density of the BMG-Machine to be lower as well. As saturation occurs at much higher magnetic field strength, these values were not obtained by the dual-coil setup but rather by means of a vibrating sample magnetometer (VSM) and thus AC-measurements.

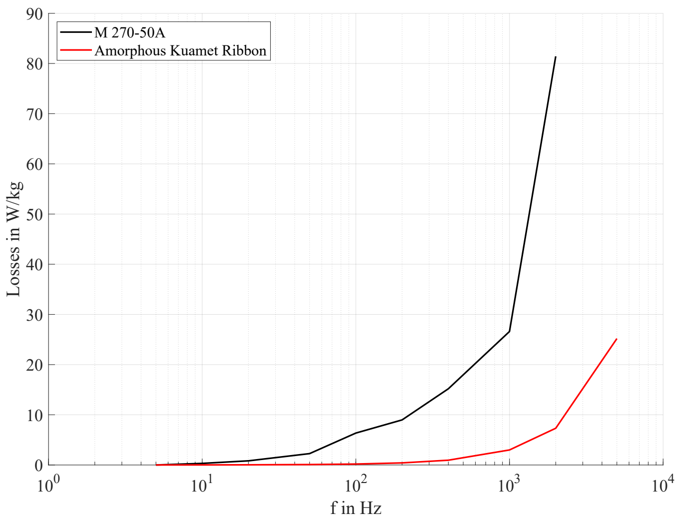


Fig. 6. Specific losses depending on the actuation frequency for both materials investigated. The peak polarization is fixed at $0.5\,\mathrm{T}$.

A different aspect of interest are the specific losses as shown in Figure 6, which were also obtained via VSM. This figure shows the losses of both materials depending on the actuation frequency and with a fixed peak polarization of $0.5\,\mathrm{T}$. As mentioned in the introduction, the specific losses of the amorphous material is lower than that of the electrical steel. The main causes of this are the higher specific electrical resistance as well as the difference in sample thickness. For the used electrical steel, the manufacturer states a specific electrical resistance of $0.565\,\mu\Omega\,\mathrm{m}$ while the amorphous material has a resistance of about $1.782\,\mu\Omega\,\mathrm{m}$ [5].

## III. Experimental Investigation

### A. Testing Environment

For testing purposes, a custom made test bench from the company IMC Messtechnik is used as shown in Figure 7. Figure 8 illustrates the same test bench abstracted as a block diagram. The load or test bench motor is controlled using the computer and its respective software while the test motor is controlled by a custom driving electronics based on a STM H7 microcontroller.

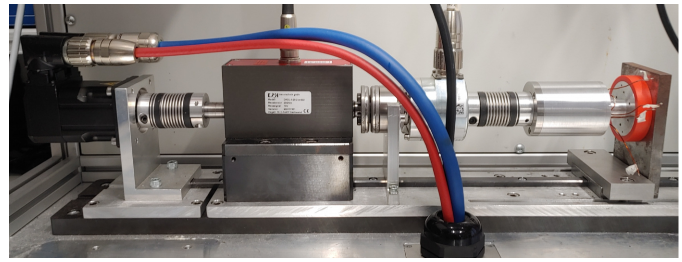

Fig. 7. Test bench used to perform the measurements. The load motor (black) is on the left, the torque sensor (gray) is in the center and the encoder is to the right of the torque sensor behind the cables. The device under test is on the right.

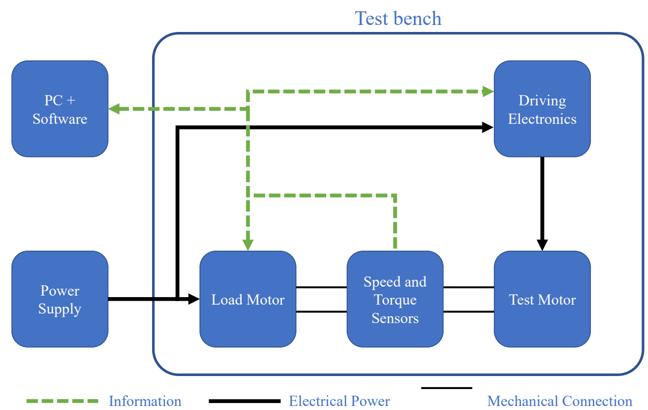


Fig. 8. Block diagram of the test bench used to perform the measurements.

With the aim of fully characterising the PMSMs, an automated measurement campaign was applied to both machines. After an initial setup procedure, the load motor is controlled to a constant speed of $100\,\mathrm{rpm}$. Subsequently, the q-axis current $i_q$ of the PMSM to be investigated is increased from $0\,\mathrm{A}$ to $12\,\mathrm{A}$ in $0.25\,\mathrm{A}$ steps. As the coils are identical for both machines, this results in the same actuation current density. Each parameter combination is applied for $5\,\mathrm{s}$ and the resulting torque is measured and averaged. Afterwards, $i_q$ is reset to $0\,\mathrm{A}$ and the speed is increased by $100\,\mathrm{rpm}$. This procedure is repeated up to a speed of $5000\,\mathrm{rpm}$. In addition to measuring the torque, the phase currents and voltages of the test motor are measured and transformed to d and q-axis values. These are used to calculate the electrical power $P_{\mathrm{el}}$ by means of

$$P_{\mathrm{el}} = V_{\mathrm{q}} i_{\mathrm{q}} + V_{\mathrm{d}} i_{\mathrm{d}}, \tag{1}$$

where $V_{\mathrm{q}}$ and $i_{\mathrm{q}}$ are the q-axis voltage and current while $V_{\mathrm{d}}$ and $i_{\mathrm{d}}$ are the d-axis voltage and current. The mechanical power $P_{\mathrm{mech}}$ of each driving state may be calculated using the measured average torque $T$ and speed $n$ using

$$P_{\mathrm{mech}} = 2\pi T n. \tag{2}$$

## B. Results

Figure 9 shows the speed-torque characteristic of both PMSMs tested for the maximum q-axis current of 12 A. Already from this figure it is obvious that there is a major difference between the two machines as the torque of the BMG-Machine is quite a bit lower than that of the Sheet-Machine. This was to be expected from the material properties, as the saturation polarization of the amorphous material is significantly smaller. Consequently, the air gap flux density of the BMG-Machine is lower as well as the resulting torque. As the polarization of the BMG is higher than that of the electrical steel at low magnetic field strengths, it is expected that the torque output of the BMG-Machine is higher if driven in this condition. However, finite element analysis has shown that the operating point of the SMCs is outside of this range due to the offset caused by the permanent magnets. Thus, this PMSM, and likely permanent magnet based machines in general, is not ideal for the BMG.

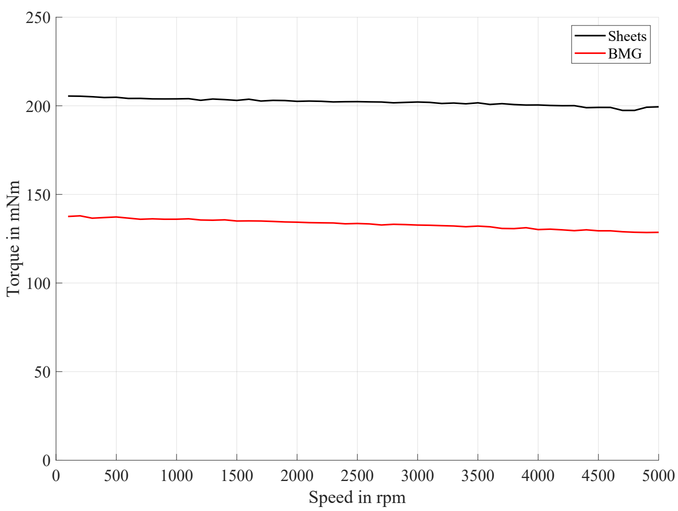


Fig. 9. Speed-Torque Characteristic of both PMSMs for $i_\text{q} = 12$ A.

Calculating the electrical power according to (1) leads to Figure 10 for the Sheet-Machine, while Figure 11 shows the electrical power of the BMG-Machine. An interesting observation is that the maximum electrical power of the BMG-Machine is lower than that of the Sheet-Machine. This can be attributed to the lower phase inductances of the BMG-Machine which were measured to be between 23.3 µH and 32.3 µH depending on the rotor position compared to 38.2 µH to 50.3 µH in the case of the Sheet-Machine. Although initially counter-intuitive as the permeability of the BMG was shown to be higher, this is only true for low magnetic field strengths. However, as mentioned earlier, this state is impossible to reach in this specific machine due to the permanent magnets. This difference in electrical power is correlated by the fact that the mechanical power at the respective current is significantly lower, too, due to the reduced torque output. As the mechanical power is simply the multiplication of the speed and torque axis, they are omitted for brevity. Dividing the respective mechanical and electrical powers leads to the efficiency $\eta$:

$$\eta = \frac{P_\text{mech}}{P_\text{el}}. \tag{3}$$

These are illustrated in Figure 12 for the Sheet-Machine and in Figure 13 for the BMG-Machine.

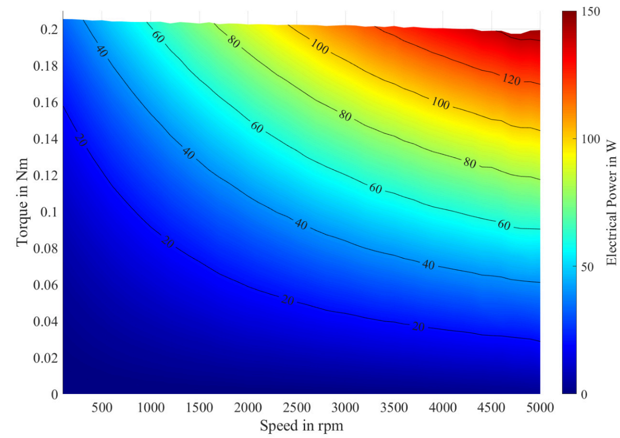


Fig. 10. Interpolated electrical power of the Sheet-Machine calculated from measured phase currents and voltages.

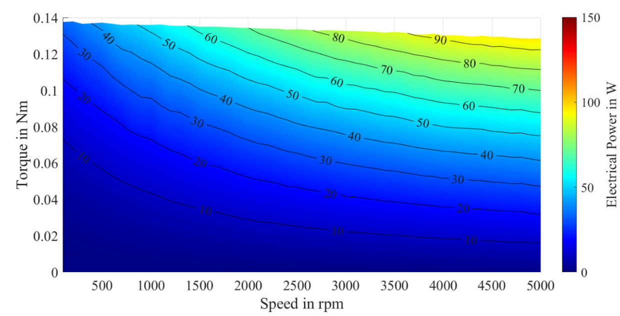


Fig. 11. Interpolated electrical power of the BMG-Machine calculated from measured phase currents and voltages.

Inspecting Figure 13 one can see that there is quite a large area indicating an efficiency of more than 80 % while the Sheet-Machine only reaches such high efficiencies at two of the investigated driving conditions. Comparing these efficiencies may be done by dividing their values at each point of interest according to

$$\eta_\text{ratio} = \frac{\eta_\text{Sheet}}{\eta_\text{BMG}}. \tag{4}$$

As the torque output is different for the two machines, the efficiency of the Sheet-Machine has to be interpolated for each data point. If the efficiency ratio $\eta_\text{ratio}$ is larger than one, the Sheet-Machine is more efficient while the BMG-Machine is more efficient for all values smaller than one. The results of (4) are shown in Figure 14.

This figure clearly shows that there is a significant range of driving conditions where the BMG-Machine is more efficient.

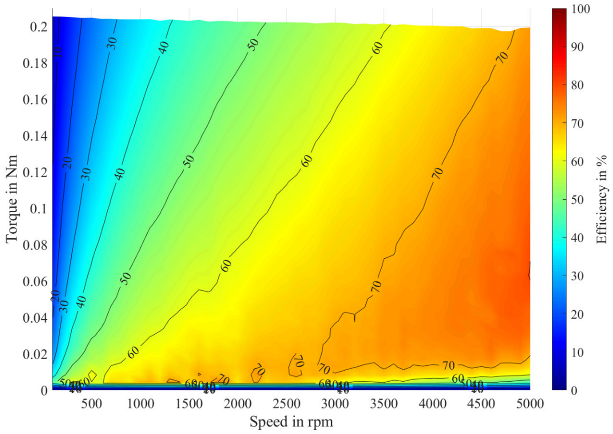


Fig. 12. Interpolated efficiency of the Sheet-Machine calculated according to (3).

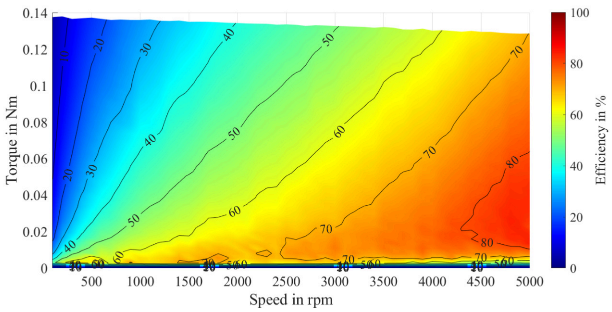


Fig. 13. Interpolated efficiency of the BMG-Machine calculated according to (3).

Although this implies that using BMG instead of laminated sheets does not simply improve the machines efficiency, it does prove that there are situations where switching to BMG components could be considered.

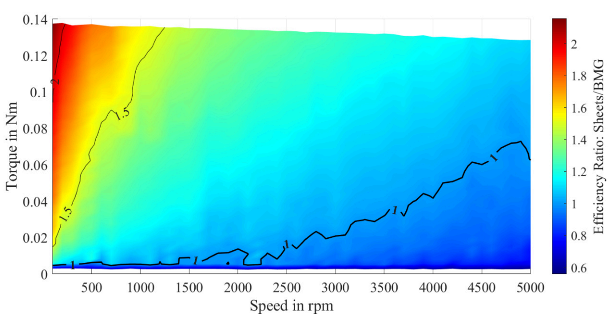


Fig. 14. Ratio of the Sheet-Machine efficiency to that of the BMG-Machine.

Another parameter that was recorded during the measurement campaign was the coil temperature using a thermocouple of type T. As the gap between a coil and the stator was too small to insert the thermocouple, it was placed on a winding head. The maximum temperature measured at each speed is illustrated in Figure 15 for both machines. Clearly, the BMG-Machine exhibits a higher temperature than the Sheet-Machine. This is especially interesting because the measurement campaign was automated and identical for both machines. Thus, the BMG-Machine should be continuously driven at lower currents than the Sheet-Machine in order to e.g., not risk demagnetization of the permanent magnets. This reduces the maximum torque output of the BMG-Machine even further. The reason for this increased temperature is not yet clear but may also indicate a lower heat capacity or a lower heat transfer rate in combination with increased losses.

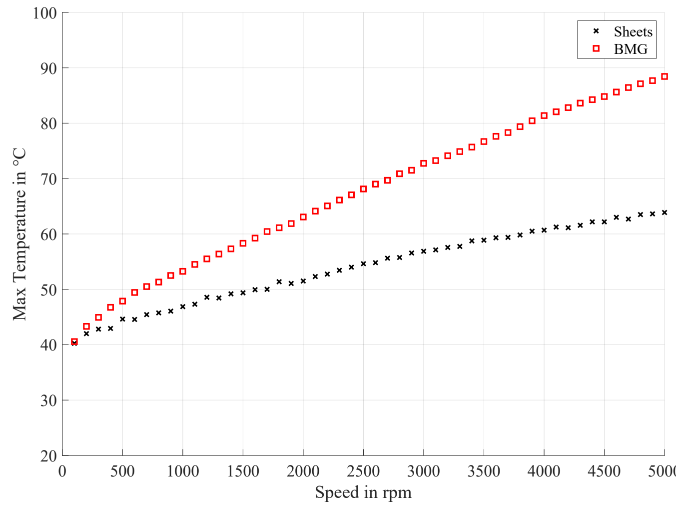


Fig. 15. Maximum measured temperature of both PMSMs at each speed for $i_q = 12\,\mathrm{A}$.

## IV. Conclusion and Outlook

This research has investigated and compared two PMSMs which are identical apart from the soft-magnetic material used. One machine was manufactured using traditional laminated sheets of electrical steel while the other machine implements soft-magnetic components made of BMG using the additive manufacturing technique SLM.

The Sheet-Machine showed a higher torque output due to its higher saturation polarization and thus an increased air gap flux density. However, the BMG-Machine was shown to have a higher efficiency than the Sheet-Machine within a region of driving conditions characterised by high speed and low torque.

In order to increase the viability of BMG in electrical machines, new soft-magnetic alloys have to be designed and investigated with the aim of increasing the saturation polarization and therefore the torque per ampere of the machine. Additionally, the alloy should exhibit a high GFA which increases the processibility for SLM. Other research topics of interest are the mechanical properties of the material as well as reducing the temperature of the machine which was shown to be significantly higher compared to the Sheet-Machine. The latter point may be approached by reducing the eddy current losses using appropriate structures instead of manufacturing the component in bulk. The SLM process could benefit from further development as well. Research could aim for higher cooling rates that might be achieved by improved process parameters, hardware and software upgrades of the equipment, or combinations thereof.

## Acknowledgment

The authors acknowledge the European Union's Horizon Europe Pathfinder-Open Programme for funding the AM2SoftMag project. Sincere appreciation goes to the National Metrology Institute of Italy (INRiM) for performing the magnetic investigation of the amorphous ribbons. R. Busch and A. Ghavimi of the Chair of Metallic Materials of Saarland University are acknowledged for providing the DSC results of the BMG stator and rotor. The authors thank Heraeus AMLOY Technologies GmbH for providing the AM-built soft-magnetic components used in the experimental investigation. Gratitude goes to I. Gallino for useful discussions and funding acquisition.

## References

[1] A. Plotkowski, K. Carver, F. List, J. Pries, Z. Li, A. M. Rossy, and D. Leonard, "Design and performance of an additively manufactured high-si transformer core," *Materials & Design*, vol. 194, p. 108894, 2020.

[2] A. D. Goodall, F. Nishanth, E. L. Severson, and I. Todd, "Loss performance of an additively manufactured axial flux machine stator with an eddy-current limiting structure," *Materials Today Communications*, vol. 35, p. 105978, 2023.

[3] F. Nishanth, A. D. Goodall, I. Todd, and E. L. Severson, "Characterization of an axial flux machine with an additively manufactured stator," *IEEE Transactions on Energy Conversion*, vol. 38, no. 4, pp. 2717–2729, 2023.

[4] H.-J. Pyo, J. W. Jeong, J. Yu, D.-W. Nam, S.-H. Yang, and W.-H. Kim, "Eddy current loss reduction in 3d-printed axial flux motor using 3d-printed smc core," in *2020 IEEE Energy Conversion Congress and Exposition (ECCE)*, pp. 1121–1125, 2020.

[5] L. Thorsson, M. Unosson, M. Teresa Pérez-Prado, X. Jin, P. Tiberto, G. Barrera, B. Adam, N. Neuber, A. Ghavimi, M. Frey, R. Busch, and I. Gallino, "Selective laser melting of a fe-si-cr-b-c-based complex-shaped amorphous soft-magnetic electric motor rotor with record dimensions," *Materials & Design*, vol. 215, p. 110483, 2022.

[6] W. Wang, C. Dong, and C. Shek, "Bulk metallic glasses," *Materials Science and Engineering: R: Reports*, vol. 44, no. 2, pp. 45–89, 2004.

[7] M. E. McHenry, M. A. Willard, and D. E. Laughlin, "Amorphous and nanocrystalline materials for applications as soft magnets," *Progress in Materials Science*, vol. 44, no. 4, pp. 291–433, 1999.

[8] H. Liebermann and C. Graham, "Production of amorphous alloy ribbons and effects of apparatus parameters on ribbon dimensions," *IEEE Transactions on Magnetics*, vol. 12, no. 6, pp. 921–923, 1976.

[9] R. Kolano, A. Kolano-Burian, M. Polak, and J. Szynowski, "Application of rapidly quenched soft magnetic materials in energy-saving electric equipment," *IEEE Transactions on Magnetics*, vol. 50, no. 4, pp. 1–4, 2014.

[10] R. Kolano, A. Kolano-Burian, K. Krykowski, J. Hetmańczyk, M. Hreczka, M. Polak, and J. Szynowski, "Amorphous soft magnetic core for the stator of the high-speed pmbldc motor with half-open slots," *IEEE Transactions on Magnetics*, vol. 52, no. 6, pp. 1–5, 2016.

[11] Z. Wang, R. Masaki, S. Morinaga, Y. Enomoto, H. Itabashi, M. Ito, and S. Tanigawa, "Development of an axial gap motor with amorphous metal cores," *IEEE Transactions on Industry Applications*, vol. 47, no. 3, pp. 1293–1299, 2011.

[12] S. Sun, F. Jiang, T. Li, B. Xu, and K. Yang, "Comparison of a multi-stage axial flux permanent magnet machine with different stator core materials," *IEEE Transactions on Applied Superconductivity*, vol. 30, no. 4, pp. 1–6, 2020.

[13] T. Kauder and K. Hameyer, "Performance factor comparison of nanocrystalline, amorphous, and crystalline soft magnetic materials for medium-frequency applications," *IEEE Transactions on Magnetics*, vol. 53, no. 11, pp. 1–4, 2017.

[14] B. Li, J. G. Zhu, C. Liu, Y. Li, F. Zhao, and Q. Jiang, "Design and comparative study of ultrahigh-speed permanent magnet motors with different soft magnetic materials," *IEEE Transactions on Magnetics*, vol. 59, no. 11, pp. 1–5, 2023.

[15] L. Petrescu, E. Cazacu, V. Ioniţă, and C. Petrescu, "Characterization of soft magnetic materials in a wide range of frequencies," in *2014 International Symposium on Fundamentals of Electrical Engineering (ISFEE)*, pp. 1–6, 2014.

[16] C. Suryanarayana and A. Inoue, "Iron-based bulk metallic glasses," *International Materials Reviews*, vol. 58, no. 3, pp. 131–166, 2013.

[17] S. Pauly, L. Löber, R. Petters, M. Stoica, S. Scudino, U. Kühn, and J. Eckert, "Processing metallic glasses by selective laser melting," *Materials Today*, vol. 16, no. 1, pp. 37–41, 2013.

[18] M. G. Özden, F. S. Freeman, and N. A. Morley, "Soft-magnetic behavior of fe-based nanocrystalline alloys produced using laser powder bed fusion," *Advanced Engineering Materials*, vol. 25, no. 19, p. 2300597, 2023.

[19] A. D. Goodall, L. Chechik, R. L. Mitchell, G. W. Jewell, and I. Todd, "Cracking of soft magnetic fesi to reduce eddy current losses in stator cores," *Additive Manufacturing*, vol. 70, p. 103555, 2023.

**Carsten Klein** was born in St. Ingbert, Germany. He received his Bachelors and Masters degree in Systems Engineering at Saarland University, Germany in 2019 and 2022 respectively.

Since then he works as a doctoral student in Systems Engineering at the Laboratory of Actuation Technology, Saarland University.

The research activities of Mr. Klein concern novel soft magnetic materials in electrical machines as well as condition monitoring and sensorless control of electromagnetic actuators.

**Lena Thorsson** was born in Sweden in 1972. She studied powder metallurgy and materials science and engineering at the Royal Institute of Technology in Stockholm (KTH), and received her Master of Science degree in 2000.

During her more than 25 years in manufacturing industry in various roles in research and development, she has worked at companies ranging from start-ups to globally established EOS GmbH, ABB AB, and Westinghouse. Her main focus has been within metal additive manufacturing (AM) and more specifically process development for laser-based powder bed fusion.

Since 2001, her main contributions to AM industry have been early work on nickel-based super-alloys, precious metals, and since 2016 on AM processes for amorphous soft-magnetic alloys.

**Christopher May** May was born in Manila, Philippines in 1967. He received his Bachelor of Science degree in mechanical engineering from the University of New Mexico, Albuquerque, in 1991.

From 1993 to 2012, he researched and developed unconventional field-controlled actuators at the Laboratory of Process Automation, Saarland University, Germany. During this time, he made defining contributions including scientific coordination to numerous European funded collaborative RTD projects investigating the application potential of magnetostrictive and other actuation technologies in aeronautic and robotic structures. Since 2012, Chris May is a scientific assistant at the Laboratory of Actuation Technology contributing to the ongoing research in the field of low-power electrical machines.

He currently supports the project coordination and implementation of the European AM2SoftMag project in which novel glassy alloys are being developed for 3D printing of soft-magnetic components for electrical machines.

**Matthias Nienhaus** was born 1963 in Wessum, Germany. He studied precision engineering at the Fachhochschule Furtwangen and electrical engineering at the University of Erlangen-Nürnberg. In 1998, he obtained his doctoral degree at the Institute for Microtechnology Mainz (IMM).

His professional carrier lead him through Bosch, Siemens, IMM (head of precision engineering department), mymotors & actuators GmbH (shareholder and managing director) and Faulhaber (area director microsystems) to his current position as full professor at the Saarland University and head of the Laboratory of Actuation Technology (LAT) since 2010.

At the LAT department he teaches and conducts research in the field of small and micro electromagnetic drives with main focus on embedded drive systems and sensorless control processes. Moreover, he leads research activities in the field of electromagnetic motor design and technology for efficient low-power mechatronic devices and systems.